

## Fiber Ablation in the Solid-Deuterium Z Pinch

Irvin R. Lindemuth and Gene H. McCall

*Inertial Fusion and Plasma Theory Group, Applied Theoretical Physics Division,  
Los Alamos National Laboratory, Los Alamos, New Mexico 87545*

Richard A. Nebel

*Plasma Theory and Computation Group, Controlled Thermonuclear Research Division,  
Los Alamos National Laboratory, Los Alamos, New Mexico 87545*

(Received 19 August 1988)

We have performed one-dimensional magnetohydrodynamic computer calculations of the formation and evolution of the solid-deuterium-fiber Z pinch. With use of a tabulated atomic data base and "cold-start" initial conditions, our computations show that current is carried by hot plasma which has been ablated from the solid fiber. The computations suggest that the experimentally observed instability growth may coincide with the complete ablation of the central fiber.

PACS numbers: 52.55.Ez, 52.25.Jm, 52.30.Jb, 52.65.+z

The linear Z pinch, in which a hot plasma is magnetically confined by the magnetic field from current passing through the plasma column, has been of interest in controlled fusion research for three decades or more. However, magnetohydrodynamic instabilities led to the abandonment of the Z pinch as a fusion system in favor of more complicated field topologies. Prompted by the advent of high-voltage pulsed power technology and stimulated by studies<sup>1,2</sup> that suggested that a high-density Z pinch could form a very compact, high- $Q$  fusion system, a series of laser-initiated, gas-embedded, Z-pinch experiments were performed at Los Alamos and elsewhere in the late 1970's and early 1980's. At Los Alamos, plasma temperatures as high as 1 keV were observed<sup>3</sup> and sustained temperatures of 200 eV with  $n_e \tau > 2 \times 10^{13}$  sec/cm<sup>3</sup> were obtained.<sup>4</sup> Concurrent with the experimental effort was the development of complex computer codes capable of modeling the observed experimental phenomena, and the experimental observations were reproduced computationally to a very satisfactory degree.<sup>5,6</sup> Experimental and computational investigations led to the conclusion that mass accretion from the cold, embedding gas into the hot plasma channel increased the line density of the pinch and limited the temperature which could be achieved.<sup>7</sup>

The gas-embedded Z-pinch work prompted the suggestion that frozen fibers, which by definition would be free from any accretion processes, could possibly be driven to fusion conditions by modern high-voltage, pulsed power generators.<sup>3,8</sup> Experiments at Los Alamos<sup>9,10</sup> and the Naval Research Laboratory (NRL)<sup>11</sup> have now demonstrated that interesting plasmas can be created from frozen deuterium fibers, and existing facilities are being upgraded to provide higher current and  $dI/dt$ . Sethian *et al.*<sup>11</sup> have reported the remarkable observation that a fiber-formed column remains stable until the driving electrical current reaches a peak, at which

time a sudden, rapid expansion and onset of neutron production is observed; it is suggested that the decreasing  $dI/dt$  leads to  $m=0$  unstable behavior.

In this paper, we report the first application of our computational capability,<sup>5,6</sup> which was developed in conjunction with the laser-initiated Z-pinch effort, to a study of the solid-deuterium-fiber Z pinch. In our computer calculations, we solve, using implicit numerical methods, the one-dimensional equations of magnetohydrodynamics which include thermal conduction and resistive diffusion. The magnetohydrodynamic model used requires for completeness the specific internal energy, the pressure, the thermal conductivity, the average ionization level, and the electrical resistivity as functions of the density and temperature. To obtain the equation of state (specific energy and pressure), the ionization level, and the resistivity, we use the Los Alamos SESAME<sup>12</sup> tabulated atomic data base computer library. The thermal conductivity uses essentially the Braginskii<sup>13</sup> formalism. In the course of a typical computation, all quantities will vary by several orders of magnitude.

The "cold-start" initial conditions for the computations reported here are a solid, cryogenic fiber [ $\rho_f = (0.5-1)\rho_s = 88-176$  kg/m<sup>3</sup>;  $T_f = 0.001$  eV] surrounded by a low density, "warm" halo ( $\rho_h = 0.176$  kg/m<sup>3</sup>;  $T_h = 1$  eV). The warm halo is required to provide an initial current conduction path, since the high-density, central fiber is an insulator at low temperature; whereas we have successfully modeled<sup>5,6</sup> the electrical breakdown process in the gas-embedded Z pinch, we have yet to formulate a model of the breakdown of the solid fiber. Typically, the radius,  $r_h$ , of the halo region is 20-30  $\mu$ m larger than the fiber radius,  $r_f$ . Parameter studies have shown that our computed results are insensitive to the value of the halo radius, even if the halo radius is as large as 7.5 times the initial fiber radius, except for a short-lived (10 ns) tran-

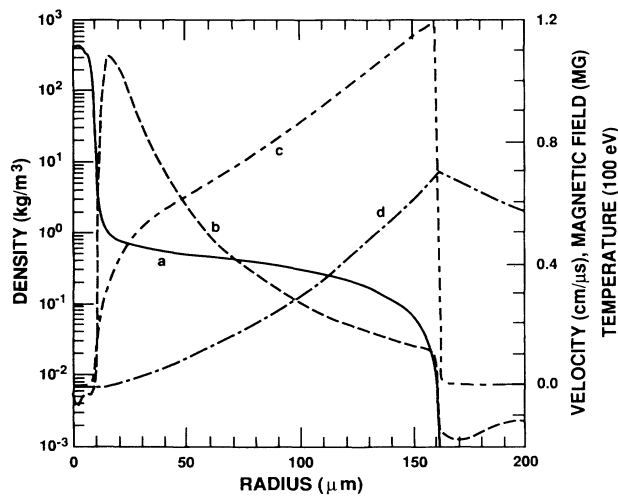


FIG. 1. Radial profiles at 35 ns for  $\rho_f = \rho_s$ ,  $r_f = 15 \mu\text{m}$ : curve *a*, mass density; *b*, radial velocity; *c*, temperature; *d*, magnetic field.

sient, because of the small mass involved.

Our computations completed to date have been primarily aimed at modeling the Los Alamos prototype experiment<sup>9,10</sup> ( $V=600$  kV,  $I=250$  kA,  $dI/dt=2 \times 10^{12}$  A/s,  $\tau_{\text{rise}}=200$  ns,  $r_f=10\text{--}20 \mu\text{m}$ ). Shown in Fig. 1 are typical radial profiles prior to the time of complete fiber ablation. As the density profile (Fig. 1, curve *a*) and the magnetic field profile (Fig. 1, curve *d*) indicate, the current is carried by essentially fully ionized plasma at a relatively low density ( $\rho < 1 \text{ kg/m}^3$ ;  $n_e < 3 \times 10^{20}/\text{cm}^3$ ). A temperature gradient (Fig. 1, curve *c*) exists across the channel, and heat is conducted radially inward to the cold fiber. The heating of the high-density fiber creates a large pressure at the fiber boundary. The large pressure causes the heated fiber material to expand radially, i.e., to ablate, at a velocity of  $1.1 \text{ cm}/\mu\text{s}$  (Fig. 1, curve *b*). In addition, the large pressure generates shock waves which propagate radially inward through the fiber and which are eventually reflected from the axis. The waves which reverberate through the fiber heat the fiber somewhat, but they are insufficient to raise the electrical conductivity of the fiber to the point where it conducts electrical current, and so the interior of the fiber is free of magnetic field (Fig. 1, curve *d*).

The computations shown in Fig. 1 are summarized in Fig. 2, which gives the temporal history of the density and temperature at various radial positions. As shown in Fig. 2, curve *a*, the density on-axis is constant at its initial value until the first shock reaches the axis within about 10 ns after current initiation. Subsequently, after a series of reverberations, the material on-axis is compressed by a factor of 4 until, at about 93 ns, the density on-axis drops abruptly. The abrupt drop by a factor of 400 corresponds, of course, to complete ablation of the fiber, after which all the material is fully ionized, as indi-

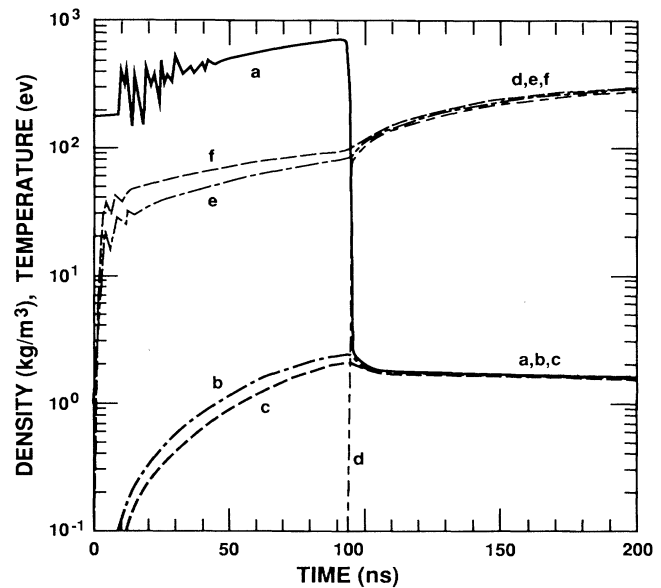


FIG. 2. Temporal history of mass density (curves *a,b,c*) and temperature (curves *d,e,f*): *a,d*, on-axis; *b,e*, at  $r=25 \mu\text{m}$ ; *c,f*, at  $r=50 \mu\text{m}$ .

cated in Fig. 2, curves *d-f*. Once the fiber has been ablated, the radial profiles change abruptly from those shown in Fig. 1 to profiles similar to those given by a similarity solution<sup>14</sup>: The temperature is uniform (Fig. 2, curves *d-f*), and the density drops off approximately parabolically (beyond the  $50\text{-}\mu\text{m}$  radius shown in Fig. 2, curves *c* and *f*). Perhaps most significantly, the radial

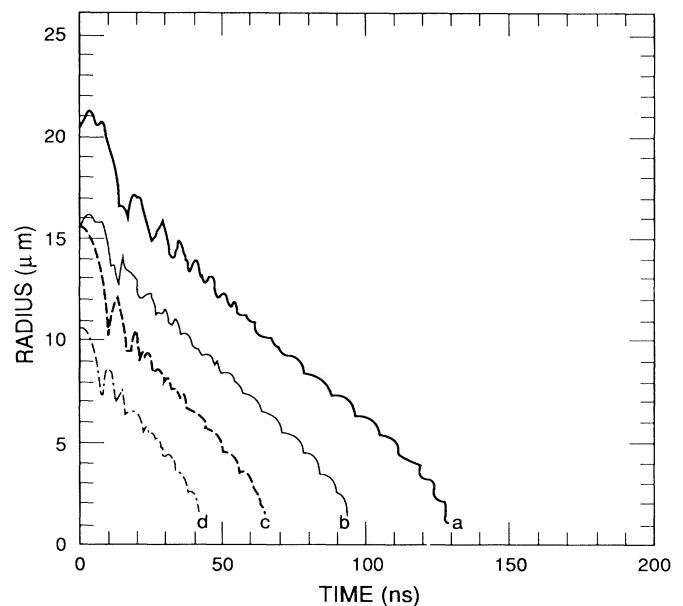


FIG. 3. Temporal history of fiber radius for, curve *a*,  $\rho_f = \rho_s$ ,  $r_f = 20 \mu\text{m}$ ; *b*,  $\rho_f = \rho_s$ ,  $r_f = 15 \mu\text{m}$ ; *c*,  $\rho_f = 0.5\rho_s$ ,  $r_f = 15 \mu\text{m}$ ; *d*,  $\rho_f = 0.5\rho_s$ ,  $r_f = 10 \mu\text{m}$ .

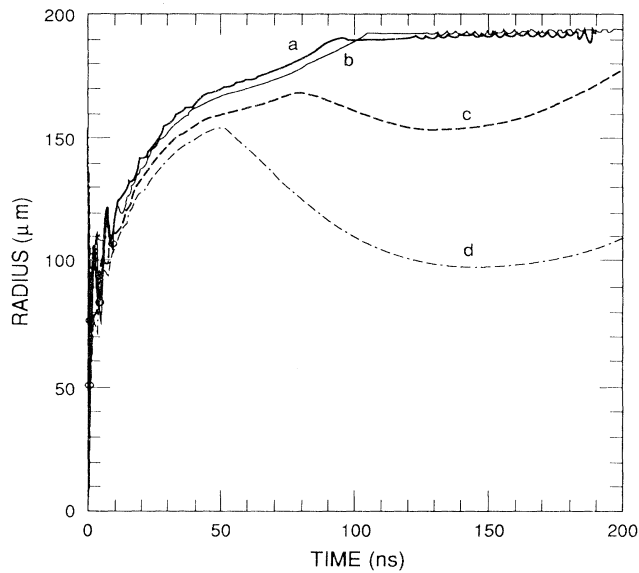


FIG. 4. Temporal history of channel radius for, curve *a*,  $\rho_f = \rho_s$ ,  $r_f = 20 \mu\text{m}$ ; *b*,  $\rho_f = \rho_s$ ,  $r_f = 15 \mu\text{m}$ ; *c*,  $\rho_f = 0.5\rho_s$ ,  $r_f = 15 \mu\text{m}$ ; *d*,  $\rho_f = 0.5\rho_s$ ,  $r_f = 10 \mu\text{m}$ .

velocity of all material drops essentially to zero, and the outward flow indicated by Fig. 1, curve *b*, ceases.

A series of computations for the Los Alamos prototype is summarized in Figs. 3 and 4. The fiber radius (Fig. 3) is the location where the density is 10% of the density on-axis. The channel radius (Fig. 4) is the location where the enclosed current is 90% of the total. The variation in the fiber radius,  $r_f$ , in Figs. 3 and 4 covers the range used in the Los Alamos experiments, and the variation in the initial density  $\rho_f$  reflects the fact that the average density of the fiber may be as low as half the solid density because of voids and other nonuniformities.<sup>15</sup> The time to complete fiber ablation ranges from 40 ns (Fig. 3, curve *d*) to 130 ns (Fig. 3, curve *a*), and the time to fiber ablation is given approximately by the expression

$$\tau_f = 6.4r_f(\rho_f/\rho_s)^{0.5},$$

where  $\tau_f$  is in ns,  $r_f$  is in  $\mu\text{m}$ , and  $\rho_s$  is the solid deuterium density ( $176 \text{ kg/m}^3$ ). In all cases, the channel radius (Fig. 4) is significantly larger than the initial fiber radius. The degree to which the channel recompresses after the fiber has ablated depends upon the fiber parameters (Fig. 4, curves *c* and *d*; the late-time constancy of Fig. 4, curves *a* and *b*, indicates proximity to the boundary of the computational domain).

Although the NRL experiments<sup>11</sup> have a higher current rise time and higher current ( $dI/dt = 4 \times 10^{12} \text{ A/s}$ ,  $I = 500 \text{ kA}$ ) than the Los Alamos prototype, the initial fiber radius is also larger ( $r_f = 40\text{--}62.5 \mu\text{m}$ ). Summarized in Fig. 5 is a computation using the NRL driving current and a solid density fiber which has an initial ra-

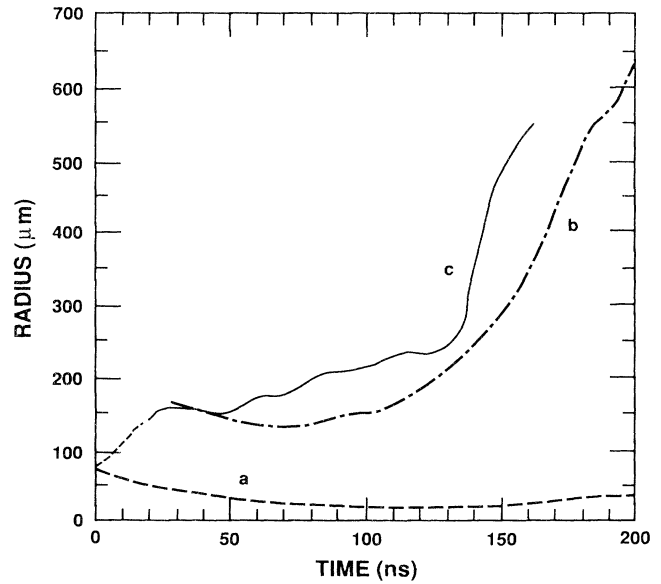


FIG. 5. Temporal history for parameters of the NRL experiment: curve *a*, computed fiber radius; *b*, computed channel radius; *c*, experimental streak-photograph radius (see Ref. 11).

dius of  $62.5 \mu\text{m}$ . Perhaps surprisingly, the fiber, although reduced to less than 50% of its initial radius, persists for the duration of the experiment (Fig. 5, curve *a*). After an initial transient, the computed current-channel radius (Fig. 5, curve *b*) is comparable to the experimentally obtained streak-photograph radius (Fig. 5, curve *c*), except for an approximately 20-ns time delay, although the rapid expansion which occurs beyond peak current is not as abrupt in the computation.

The agreement between the computed current channel (Fig. 5, curve *b*) and the experimentally measured radius (Fig. 5, curve *c*) would appear to confirm our computational prediction that the solid fiber persists significantly longer in existing experiments<sup>9-11</sup> than previously expected. However, experimental techniques to definitively detect the presence or absence of the fiber have not yet been developed.

Our one-dimensional computations do not provide an explanation of the onset of neutron production observed in the NRL experiments. McCall<sup>16</sup> has formulated a simple model of  $m=0$  unstable behavior which predicts the observed scaling of the neutron output with current; *a priori* it appears that McCall's mechanism would not apply until the fiber has totally ablated. Preliminary cold-start, two-dimensional computations<sup>17</sup> indicate that the low-density plasma outside the fiber undergoes  $m=0$  behavior as early as 10 ns and that the  $m=0$  behavior can somewhat increase the fiber ablation rate. Hence, Fig. 5, McCall's model,<sup>16</sup> and our preliminary two-dimensional computations<sup>17</sup> prompt the speculation that the fiber ablation process may play an important role in the stability of the pinch and that neutron production

may occur at the time of complete fiber ablation. This conjecture is consistent with Los Alamos observations<sup>10</sup> of  $m=0$  modes at a time comparable to the fiber ablation time of Fig. 3, curves *b* and *c*.

Although the computations reported here do not include radiative effects, "two-temperature" computations using SESAME<sup>12</sup> opacities to couple radiation to the plasma show no significant differences from the computations of this paper. We are now assessing the validity of the entire atomic data base which is required in the computations. We are also applying a variety of computational tools to address the role of thermal conduction, resistive diffusion, viscous dissipation, and driving-current wave form on the stability and evolution of the pinch.

The authors would like to acknowledge stimulating discussions with C. Fenstermacher, J. Hammel, E. Lindman, R. Lovberg, D. Mosher, P. Sheehy, D. Scudder, J. Sethian, and J. Shlachter. This work was performed under the auspices of the U.S. Department of Energy. Los Alamos National Laboratory is operated by the University of California for the United States Department of Energy under Contract No. W-7405-ENG-36.

---

<sup>1</sup>J. E. Hammel, Los Alamos National Laboratory Report No. LA-6203-MS, 1976 (unpublished).

<sup>2</sup>R. L. Hagenson, A. S. Tai, R. A. Krakowski, and R. W. Moses, *Nucl. Fusion* **21**, 1351 (1981).

<sup>3</sup>J. E. Hammel, D. W. Scudder, and J. S. Shlachter, in *Proceedings of the First International Conference on Dense Z-Pinches for Fusion*, edited by J. D. Sethian and K. A. Gerber (Naval Research Laboratory, Washington, D.C., 1984), p. 13.

<sup>4</sup>L. A. Jones, K. H. Finken, A. Dangor, E. Kallne, S. Singer, I. R. Lindemuth, J. H. Brownell, and T. A. Oliphant, *Appl. Phys. Lett.* **38**, 522 (1981).

<sup>5</sup>I. R. Lindemuth, J. H. Brownell, T. A. Oliphant, and D. L. Weiss, *J. Appl. Phys.* **53**, 1415 (1982).

<sup>6</sup>I. R. Lindemuth, in Ref. 3, p. 46.

<sup>7</sup>J. S. Shlachter, J. E. Hammel, and D. W. Scudder, in Ref. 3, p. 87.

<sup>8</sup>N. R. Pereira, N. Rostoker, J. Riordan, and M. Gersten, in Ref. 3, p. 71.

<sup>9</sup>D. W. Scudder, *Bull. Am. Phys. Soc.* **30**, 1408 (1985).

<sup>10</sup>J. Hammel and D. W. Scudder, in *Proceedings of the Fourteenth European Conference on Controlled Fusion and Plasma Physics, Madrid, Spain, 1987*, edited by F. Engelmann and J. L. Alvarez Rivas (European Physical Society, Geneva, Switzerland, 1987), p. 450.

<sup>11</sup>J. D. Sethian, A. E. Robson, K. A. Gerber, and A. W. DiSilva, *Phys. Rev. Lett.* **59**, 892 (1987).

<sup>12</sup>Los Alamos National Laboratory Report No. LA-10160-MS, 1984, edited by K. S. Holian (unpublished).

<sup>13</sup>S. I. Braginskii, in *Reviews of Plasma Physics*, edited by M. A. Leontovich (Consultants Bureau, New York, 1965), Vol. 1, p. 205.

<sup>14</sup>P. Rosenau, R. A. Nebel, and H. R. Lewis, to be published.

<sup>15</sup>J. E. Hammel, private communication.

<sup>16</sup>G. H. McCall, to be published.

<sup>17</sup>I. R. Lindemuth and R. A. Nebel, *Bull. Am. Phys. Soc.* **33**, 1908 (1988).